Actin-binding protein ABP140 is a methyltransferase for 3-methylcytidine at position 32 of tRNAs in *Saccharomyces cerevisiae*

AKIKO NOMA,[1] SANGHYUN YI,[1] TAKAYUKI KATOH,[1] YOSHIMI TAKAI,[2] TAKEO SUZUKI,[1] and TSUTOMU SUZUKI[1]

[1]Department of Chemistry and Biotechnology, Graduate School of Engineering, University of Tokyo, Bunkyo-ku, Tokyo 113-8656, Japan
[2]Division of Molecular and Cellular Biology, Department of Biochemistry and Molecular Biology, Kobe University Graduate School of Medicine/ Faculty of Medicine, Kobe, Hyogo, Japan

ABSTRACT

Transfer RNAs contain various modified nucleotides that are introduced enzymatically at the post-transcriptional level. In *Saccharomyces cerevisiae*, 3-methylcytidine (m^3C) is found at position 32 of the tRNAs for Thr and Ser. We used a systematic reverse genetic approach combined with mass spectrometry (ribonucleome analysis), and identified the actin-binding protein ABP140 as the protein responsible for m^3C formation in both $tRNA^{Thr1}$ and $tRNA^{Ser1}$. ABP140 consists of an N-terminal actin-binding sequence and a C-terminal S-adenosylmethionine (Ado-Met) binding motif. Deletion of the actin-binding sequence in ABP140 did not affect m^3C formation, indicating that subcellular localization of ABP140 to actin filaments is not involved in tRNA modification. m^3C formation in $tRNA^{Thr1}$ could be reconstituted using recombinant Abp140p in the presence of Ado-Met, whereas m^3C did not form in $tRNA^{Ser1}$ in vitro, indicating the absence of a factor(s) required for $tRNA^{Ser1}$ m^3C formation. Thus, *ABP140* has been designated *TRM140* according to the preferred nomenclature. In addition, we observed a specific reduction of m^3C formation in HeLa cells by siRNA-mediated knock down of the human ortholog of *TRM140*.

Keywords: 3-methylcytidine; ABP140; S-adenosylmethionine; *TRM140*; tRNA

INTRODUCTION

RNA modifications play pivotal roles in the biogenesis, metabolism, structural stability, and functions of RNA molecules. To date, more than 100 chemically different, site-specific RNA modifications have been identified (Dunin-Horkawicz et al. 2006; Cantara et al. 2011). The majority of RNA modifications occur in tRNAs (Juhling et al. 2009). In particular, a wide variety of modifications in the anticodon loop of tRNAs facilitate the efficient and accurate recognition of cognate codons, and are therefore integral in protein synthesis (Bjork 1995; Curran 1998; Suzuki 2005; Agris et al. 2007).

3-methylcytidine (m^3C) (Fig. 1A) was first isolated in 1963 from soluble yeast RNA (Hall 1963). m^3C is found in both eukaryotic rRNAs and tRNAs (Iwanami and Brown 1968; Maden and Salim 1974). In *Saccharomyces cerevisiae*, m^3C is located at position 32 of $tRNA^{Thr1}$ and $tRNA^{Ser1}$ (Fig. 1B; Weissenbach et al. 1977; Olson et al. 1981). In the anticodon loop of tRNAs, residues at position 32 at the 5′ end of the anticodon loop are nearly conserved as pyrimidines (Y = U/C). Y32 forms a noncanonical base pair with the residue at position 38 (Olejniczak and Uhlenbeck 2006), which is most frequently adenosine. It has been proposed that the structure of the Y32–A38 pair is essential for the U-turn conformation of the anticodon loop. A U32C mutation in *Escherichia coli* $tRNA^{Gly}$ resulted in tighter binding to both cognate and near-cognate codons at the A-site of the ribosome (Lustig et al. 1993). Similarly, misincorporation of Ala at the near cognate GUC codon was caused by $tRNA^{Ala}$ with mutations of base pairs at positions 32 and 38 (Murakami et al. 2009). These observations clearly suggest the importance of the Y32–A38 pair of aminoacyl-tRNAs for uniform and accurate codon recognition at the A-site (Olejniczak and Uhlenbeck 2006). At the P-site of the ribosome, the C-terminal tail of the ribosomal protein S9 contacts residues 32–34 of peptidyl-tRNAs (Korostelev and

Reprint requests to: Tsutomu Suzuki, Department of Chemistry and Biotechnology, Graduate School of Engineering, University of Tokyo, Bunkyo-ku, Tokyo 113-8656, Japan; e-mail: ts@chembio.t.u-tokyo.ac.jp; fax: 81-3-5841-0550.

Article published online ahead of print. Article and publication date are at http://www.rnajournal.org/cgi/doi/10.1261/rna.2653411.

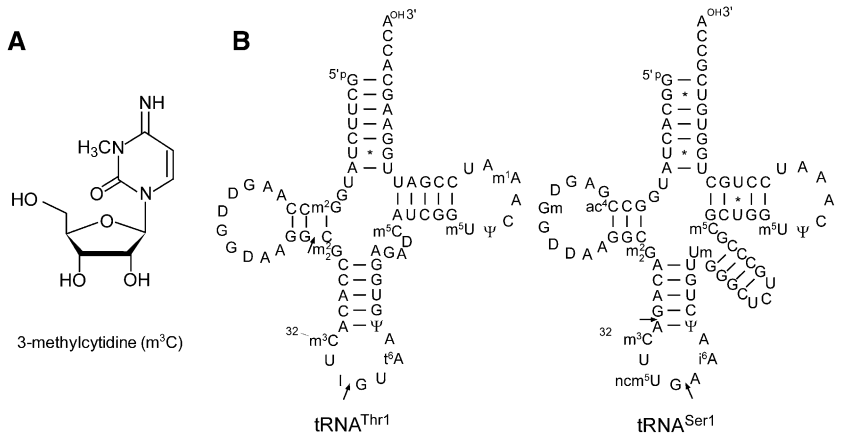

FIGURE 1. The chemical structure of 3-methylcytidine and its position in $tRNA^{Thr1}$ and $tRNA^{Ser1}$. (*A*) Chemical structure of 3-methylcytidine (m^3C). (*B*) Secondary structures of *S. cerevisiae* $tRNA^{Thr1}$ and $tRNA^{Ser1}$ with modified nucleosides: 3-methylcytidine (m^3C), N^2-methylguanosine (m^2G), dihydrouridine (D), N^2,N^2-dimethylguanosine (m^2_2G), inosine (I), N^6-threonylcarbamoyladenosine (t^6A), pseudouridine (Ψ), 5-methylcytidine (m^5C), 5-methyluridine (m^5U), 1-methyladenosine (m^1A), N^4-acetylcytidine (ac^4C), 2′-*O*-methylguanosine (Gm), 5-carbamoylmethyluridine (ncm^5U), N^6-isopentenyladenosine (i^6A), and 2′-*O*-methyluridine (Um). Arrows indicate sites of RNase T_1 cleavage to generate RNA fragments containing residues at position 32.

Noller 2007; Nasvall et al. 2009). Aberrant interaction between the C-terminal tail of S9 and residue 32 resulted in an increase in +1 frameshifting, indicating that the correct recognition of residue 32 by S9 has a critical role in reading-frame maintenance. Despite the functional importance of position 32, little is known about m^3C32. Methyl modification of m^3C32 might modulate accurate codon recognition at the A-site and the proper ribosomal positioning at the P-site. To investigate the functional roles of m^3C, it will be necessary to identify the gene or enzyme responsible for this modification.

To explore the genes responsible for tRNA and rRNA modifications, our group has developed a genome-wide screen using a reverse genetic approach combined with mass spectrometry, which we call ''ribonucleome analysis'' (Suzuki 2005; Suzuki et al. 2007). This analysis utilizes a knockout strain collection of *S. cerevisiae* (or *E. coli*). Total RNA extracted from each strain is analyzed by liquid chromatography/mass spectrometry (LC/MS) to determine whether deletion of a particular gene leads to the absence of a specific modified nucleoside, thereby permitting us to identify the enzyme or protein responsible for the modification. In the case of essential genes, temperature-sensitive mutants were cultured at the nonpermissive temperature, or expression-controlled strains were used (Soma et al. 2003). Ribonucleome analysis allows us to identify not only the enzymes directly responsible for RNA modifications, but also genes that encode proteins that lack enzymatic activity but are necessary for RNA modifications. These include carriers of the metabolic substrates used for RNA modifications and partner proteins needed for RNA recognition. Using this approach in yeast, we identified and characterized *TYW1-4* for wybutosine (Noma et al. 2006) and *URM1*, *UBA4*, *NCS2*, *NCS6*, and *TUM1* for 2-thiouridine in *S. cerevisiae* (Noma et al. 2009).

In this study we utilized ribonucleome analysis to determine the enzyme responsible for m^3C formation in $tRNA^{Thr1}$ and $tRNA^{Ser1}$, and identified *ABP140*, which encodes an actin-binding protein with previously unknown function (Asakura et al. 1998).

RESULTS

Genome-wide screening for the gene responsible for m^3C formation by ribonucleome analysis

To explore the genes responsible for tRNA modifications, including m^3C in *S. cerevisiae*, ribonucleome analysis was performed (Suzuki et al. 2007). Assuming that the gene responsible for m^3C formation was nonessential, 4829 nonessential genes in *S. cerevisiae* were examined as a parent population for screening. Because m^3C is also found in *Schizosaccharomyces pombe*, 3482 genes were selected for study, the orthologs of which are present in *S. pombe*. Finally, 351 genes whose ORFs were described as proteins of unknown function in *S. cerevisiae* (CYGD: http://mips.gsf.de/genre/proj/yeast) (Guldener et al. 2005) were chosen for ribonucleome analysis. In the mass chromatogram (Fig. 2A), m^3C was detected as a proton adduct form (MH^+; m/z 258) in wild-type cells. Among the 351 haploid knockout strains, the *yor240wΔ* was identified as a strain in which m^3C was absent (Fig. 2A). *YOR240w* encodes the latter half of a long gene named *ABP140* (Fig. 3A). *ABP140* was reported as a fused gene of *YOR239w* and *YOR240w* by connecting with the +1 frameshift site at the junction of these two genes (Asakura et al. 1998). We next examined the *yor239wΔ* strain, which lacks the former half of this gene (Fig. 3A) and found the absence of m^3C (Fig. 2A). We also constructed an *abp140Δ* strain that lacks the entire *ABP140* gene. As expected, m^3C was absent in the *abp140Δ* strain (Fig. 2A). Levels of other detectable nucleosides were normal in these strains (data not shown).

Absence of m^3C at position 32 in $tRNA^{Thr1}$ and $tRNA^{Ser1}$

To confirm the absence of m^3C at position 32 of individual tRNAs, $tRNA^{Thr1}$ and $tRNA^{Ser1}$ were isolated from both wild-type and *yor240wΔ* strains. The absence of m^3C in both tRNAs isolated from *yor240wΔ* strain was confirmed by nucleoside analysis using LC/MS (Supplemental Fig. 1). Next, each tRNA was digested into RNA fragments by

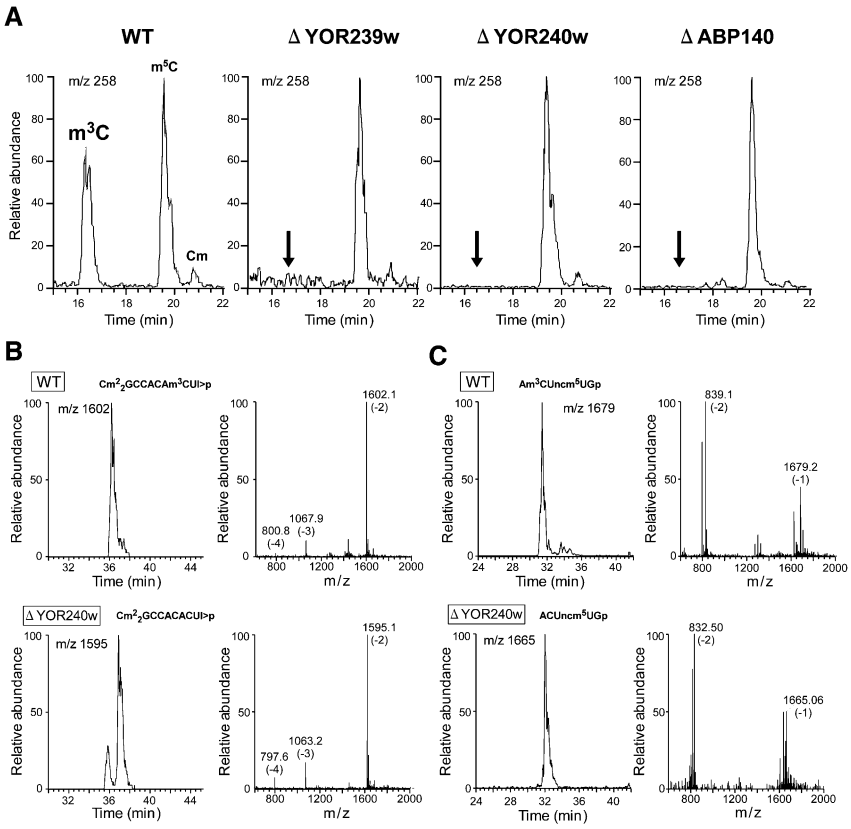

FIGURE 2. Mass spectrometric analysis of total nucleosides and individual tRNAs from *S. cerevisiae* wild-type and mutant cells. (*A*) LC/MS analysis of total nucleosides from strains of wild-type (WT), *yor239wΔ*, *yor240wΔ*, and *abp140Δ*. Graphs show mass chromatograms traced by MH^+ (m/z 258) of m^3C, m^5C, and 2′-*O*-methylcytidine (Cm). Arrows indicate the retention time for m^3C. (*B*,*C*) CapLC/nanoESI MS analysis of RNase T_1-digested $tRNA^{Thr1}$ (*B*) or $tRNA^{Ser1}$ (*C*) isolated from wild-type (*top*) and *yor240wΔ* (*bottom*) strains. (*Left*) The mass chromatograms traced by doubly charged ions of fragments bearing m^3C32 (m/z 1602 [*B*] or 1679 [*C*]) and C32 (m/z 1595 [*B*] or 1665 [*C*]). (*Right*) The mass spectra of position 32 containing fragments. The charge states of multiply charged ions are indicated in parentheses. The RNA sequences of each fragment are indicated on each graph. ''>p'' at the 3′ end of the fragment indicates cyclic phosphate. ''Relative abundance'' for *y*-axis of mass chromatograms and mass spectra shown in this figure and Figures 4, 5, and 6 stands for the percentile presentation of peak intensities that were normalized, with the highest peak defined as 100.

$RNase\ T_1$ and analyzed by capillary liquid chromatography nano electrospray mass spectrometry (CapLC/nanoESI MS) (Suzuki et al. 2007; Ikeuchi et al. 2010). In wild-type $tRNA^{Thr1}$, the RNA fragment containing position 32, $Cm^2{}_2GCCACAm^3CUI{>}p$ (MW 3206.4), was detected as doubly, triply, and quadruply charged ions (m/z 1602.1, m/z 1067.9, and m/z 800.8) as expected (Fig. 2B). The equivalent RNA fragment in $tRNA^{Thr1}$ isolated from the *yor240wΔ* strain was detected as m/z 1595.1 (a doubly charged ion) with a MW of 3192.4, which exactly matched with the molecular mass of the RNA fragment with C32 ($Cm^2{}_2GCCACACUI{>}p$). In wild-type $tRNA^{Ser1}$, the wobble base has not yet been reported (Olson et al. 1981). Therefore, nucleoside analysis was performed, which resulted in the identification of the wobble base as 5-carbamoylmethyluridine (ncm^5U) (Fig. 1B; Supplemental Fig. 1). The RNA fragment containing position 32, Am^3CUncm^5UGp (MW 1680.2), was detected as singly and doubly charged ions (m/z 1679 and m/z 839) (Fig. 2B). The equivalent RNA fragment in $tRNA^{Ser1}$ isolated from the *yor240wΔ* strain was detected as m/z 1665 (MW 1666.2), which corresponded to the molecular mass of the RNA fragment with C32 ($ACUncm^5UGp$). To confirm this result, primer extension analysis was performed to verify the absence of m^3C in $tRNA^{Ser1}$ from the *yor240wΔ* strain (Supplemental Fig. 2). In addition, both $tRNA^{Thr1}$ and $tRNA^{Ser1}$ isolated from the *yor240wΔ* strain lacked only m^3C at position 32 and retained other modifications (data not shown; pseudouridines were not analyzed).

The Ado-Met binding motif in *ABP140* is required for m^3C formation

S. cerevisiae ABP140 consists of an N-terminal actin-binding motif, a +1 frameshift site, and the C-terminal Ado-Met binding motif (Fig. 3A). When aligned with orthologs from other organisms (Fig. 3B), the C-terminal Ado-Met binding motif is conserved in budding yeast, fission yeast, *Drosophila*, and mammals, while the N-terminal region is only conserved in budding yeast, including *Candida glabrata* and *Ashbya gossypii* (Fig. 3B).

At the +1 frameshift site (Fig. 3A), the sequence CTTAGGC is a slippery sequence that can promote ~40% frameshift efficiency (Belcourt and Farabaugh 1990; Shah et al. 2002; Farabaugh et al. 2006). On the 0-frame, CTT-AGG is translated as Leu-Arg. Upon +1 frameshift, CTTA-GGC is recoded to Leu-Gly. To test whether or not the frameshift event is required for m^3C formation, the *abp140Δ* strain was transformed with a plasmid vector (WT(0-frame)) harboring *ABP140*, in which the +1 frameshift site (CTTAGGC) was replaced with the 0-frame sequence (CTTGGC). Because m^3C was efficiently formed with this construct (Fig. 4), the +1 frameshift event is not associated with m^3C formation.

Abp140p localizes to actin filaments in the cell. Next, whether or not binding of Abp140p to actin filaments is required for m^3C formation was examined. An *ABP140* mutant (delN) lacking the N-terminal actin-binding motif was constructed (Fig. 3B), and the cellular localization of delN was analyzed by fluorescent microscopy. The delN

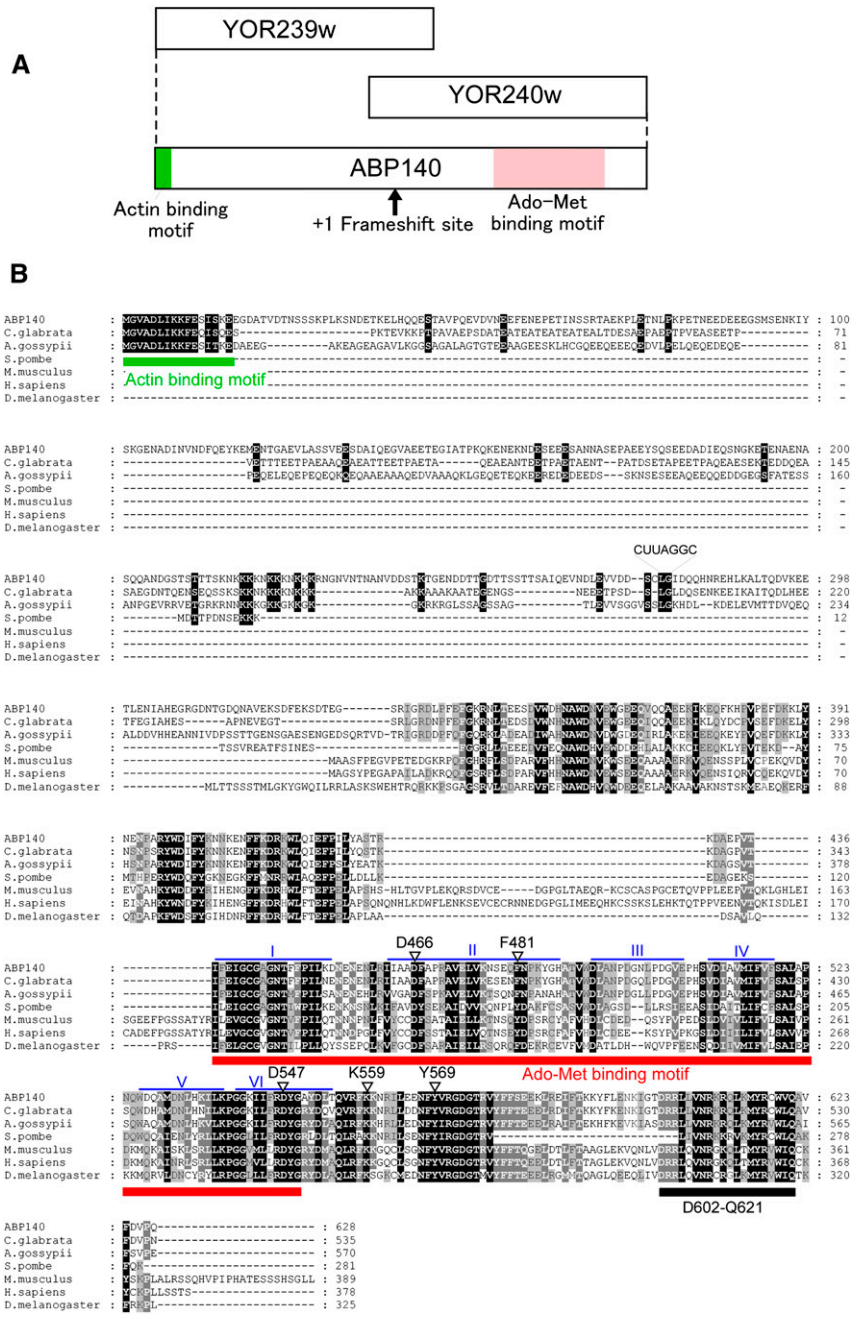

FIGURE 3. Domain structure and sequence alignment of the *ABP140/TRM140* protein and its homologs. (*A*) Domain structure of the *S. cerevisiae ABP140/TRM140* protein. Positions of *YOR239w* and *YOR240w* are shown. The actin-binding motif, +1 frameshift site, and Ado-Met binding motif are indicated. (*B*) Sequence alignment of *ABP140* and its homologs from fungi and other eukaryotes. All of these homologs were previously indicated (Farabaugh et al. 2006). The conserved actin-binding site and Ado-Met binding motif are underlined. The 7-mer slippage sequence is indicated at the +1 frameshift site. Motifs I–VI of Rossmann-fold-type class I methyltransferases are lined at the *top* of the sequence. The residues and C-terminal conserved region mutated in this study are indicated. Accession numbers are NC_006033.1 (*Candida glabrata*), NP_983532 (*Ashbya gossypii*), CAB76043.1 (*Schizosaccharomyces pombe*), BAE31989 (*Mus musculus*), NP_060866 (*Homo sapiens*), and NP_647636 (*Drosophila melanogaster*).

mutant was diffused in cytoplasm (data not shown) and, as shown in Figure 4, m^3C in the *abp140*Δ strain was efficiently formed. Therefore, localization of Abp140p to actin filaments is not necessary for m^3C formation in tRNAs.

ABP140 contains a conserved Ado-Met binding motif in its C-terminal region. To determine the role of this motif in m^3C formation, five conserved amino acids were substituted with Ala (D466A, F481A, D547A, K559A, and Y569A), and the conserved region near the C terminus was deleted (delD602-Q621) (Fig. 3B). The *abp140*Δ strain was then transformed with each of these constructs. As shown in Figure 4, no m^3C formation was observed in the D466A and delD602-Q621 mutants, and the D547A mutant showed decreased activity. Other mutants efficiently accomplished m^3C formation. These data demonstrated that the conserved Ado-Met binding motif in *ABP140* is involved in m^3C formation.

In vitro reconstitution of m^3C with recombinant Abp140p

Next, we performed in vitro reconstitution of m^3C using recombinant *ABP140* protein. A hexahistidine-tagged Abp140p was expressed in *S. cerevisiae* and purified using a Ni^{2+}-chelating column. Although the molecular weight of Abp140p was calculated to be 71.5 kDa based on its amino acid sequence, Abp140p is detected at around 140 kDa by SDS-PAGE analysis (Asakura et al. 1998). Likewise, the recombinant Abp140p was detected at ~150 kDa due to the 19-kDa C-terminal tag (Fig. 5A), indicating a homodimer formed through covalent linkage(s) other than disulfide bond. Purified Abp140p was confirmed by peptide mapping using LC/MS (data not shown). For in vitro reconstitution of m^3C, $tRNA^{Thr1}$, and $tRNA^{Ser1}$ purified from the *yor240w*Δ strain were utilized as substrate tRNAs. When $tRNA^{Thr1}$ was used as a substrate, m^3C was clearly introduced by the recombinant Abp140p in the presence of Ado-Met (Fig. 5B). On the other hand, $tRNA^{Ser1}$ was not methylated by Abp140p under the same condition as the methylation of $tRNA^{Thr1}$ (Fig. 5B), indicating that some essential factor(s) required for m^3C formation in $tRNA^{Ser1}$ was missing. Alternatively, the order of modifications may be important for m^3C32 formation in $tRNA^{Ser1}$, potentially indicating

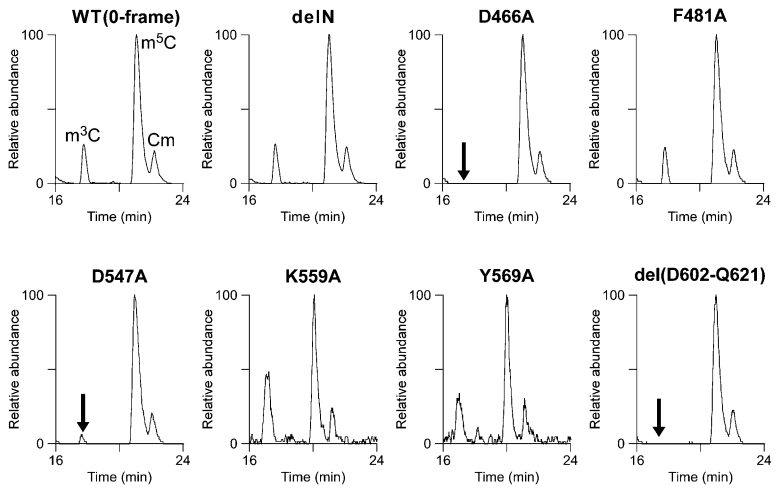

FIGURE 4. Complementation of the *yor239wΔ* strain with plasmid-encoded *ABP140* containing various mutations. LC/MS analysis of total nucleosides isolated from *yor239wΔ* strains with various *ABP140* constructs containing various mutations; WT(0-frame), delN, D466A, F481A, D547A, K559A, Y569A, and del(D602-Q621). Mass chromatograms detecting MH^+ (m/z 258) of m^3C, m^5C, and Cm are shown. Arrows indicate the retention time for m^3C.

that the introduction of other modification(s) prior to m^3C32 might inhibit m^3C32 formation. We then used unmodified $tRNA^{Ser1}$ that was transcribed in vitro using T7 RNA polymerase as a substrate for Abp140p. No m^3C32 formation activity was observed in this transcript (data not shown). Some modifications in $tRNA^{Ser1}$ might act as positive determinant for m^3C32 formation. In the case of the $tRNA^{Thr1}$ transcript, very little m^3C formation could be observed in this transcript (data not shown). This result suggested that other modifications are required for efficient m^3C32 formation in $tRNA^{Thr1}$.

These results demonstrated that Abp140p is a methyltransferase for m^3C32 of $tRNA^{Thr1}$. Therefore, Abp140p was designated as Trm140p according to the preferred nomenclature.

METTL2B is a human ortholog of Trm140p

Mammalian homologs of Trm140p were searched by BLAST with *ABP140* as a query. The search retrieved methyltransferase-like protein 2B (METTL2B) and methyltransferase-like protein 2 as human and mouse orthologs, respectively (Fig. 3B). Phylogenic analysis of these homologs were reported (Farabaugh et al. 2006). Both orthologs possess the conserved Ado-Met binding motif at the C-terminal region of *ABP140* and lack the N-terminal region of *ABP140*. To examine whether METTL2B is a methyltransferase for m^3C formation, short-hairpin(sh)RNA was used to knock down METTL2B mRNA in HeLa cells. Five days after transfection of shRNA, the cells were harvested

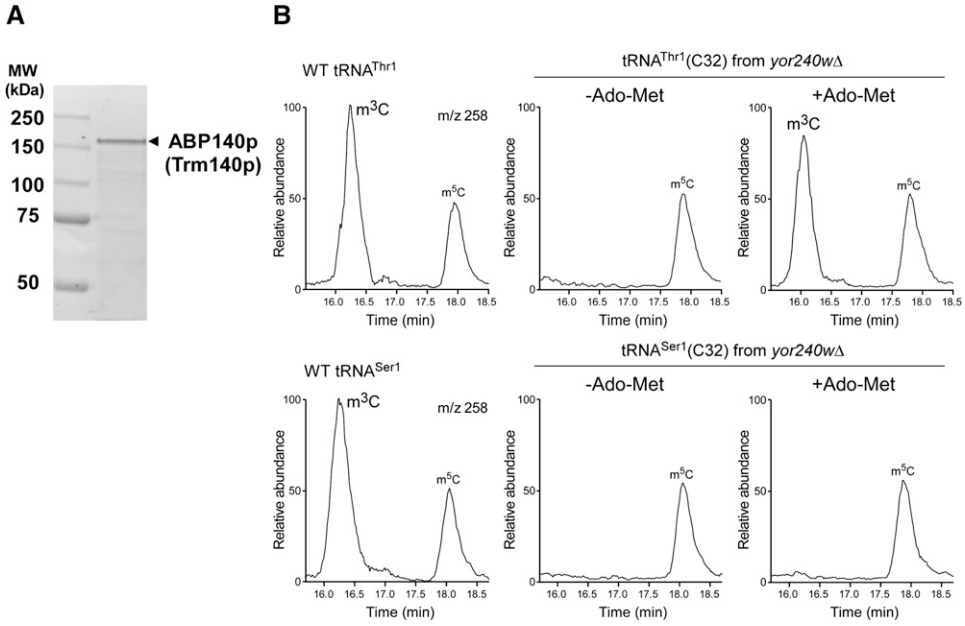

FIGURE 5. In vitro reconstitution of m^3C32 by recombinant Trm140p. (*A*) C-terminal hexahistidine-tagged recombinant Trm140p resolved on SDS-PAGE and stained with Coomassie brilliant blue (CBB). (*B*) Mass chromatograms detecting MH^+ (m/z 258) of m^3C (and m^5C) in total nucleosides from individual $tRNA^{Thr1}$ (*top left*) and $tRNA^{Ser1}$ (*bottom left*) isolated from the wild-type strain. (*Right*) The same mass chromatograms (m/z 258) of $tRNA^{Thr1}$ (*top right*) or $tRNA^{Ser1}$ (*bottom right*) in the absence (−Ado-Met) or presence (+Ado-Met) of Ado-Met.

and total RNAs were extracted. LC/MS analysis revealed that the steady-state level of m^3C was specifically decreased upon knock down of METTL2B (Fig. 6). Therefore, METTL2B was detemined to be a human homolog of Trm140p. However, there might be some partner proteins of METTL2B that are required to reconstitute m^3C formation in tRNAs. Further investigation still needs to clarify this issue.

DISCUSSION

ABP140 was first isolated as an actin-binding protein from the soluble fraction of *S. cerevisiae* (Asakura et al. 1998). Abp140p interacts with filamentous(F)-actin and has an activity to cross-link F-actin into a bundle in vitro. In the cell, Abp140p colocalizes with cortical actin patches and cytoplasmic actin filaments. However, disruption of the *ABP140* gene did not affect cell growth or organization of F-actin. The functional role of *ABP140* has been elusive. *ABP140* fused to GFP has been used as a reporter to visualize F-actin in the cell (Yang and Pon 2002). The N-terminal 17-mer peptide of *ABP140* was found to be an actin-binding motif sufficient to mediate actin localization (Riedl et al. 2008), and a chemically modified 17-mer peptide has been developed as a versatile tool by which to visualize actin dynamics in the cell (Riedl et al. 2008). Although *ABP140* shows a functional relevance to F-actin, we found no significant importance for actin localization in m^3C formation, as no effect on m^3C formation was observed upon deletion of the N-terminal actin-binding motif. In addition, in an in vitro m^3C formation in $tRNA^{Thr1}$ catalyzed by recombinant Trm140p, the addition of F-actin to the reaction mixture did not alter of m^3C-forming activity (data not shown). Taken together, the actin-binding activity of Trm140p appears to be independent of m^3C catalytic activity.

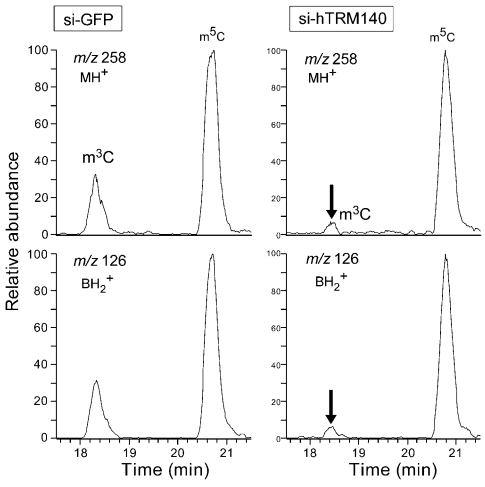

FIGURE 6. Knockdown of human *TRM140* decreases m^3C formation. LC/MS nucleoside analysis of RNA from cells treated with shRNAs targeting GFP (*left*) and hTRM140 (*right*). (*Top*, *bottom*) Mass chromatograms detecting MH^+ (m/z 258) and BH^{2+} (m/z 126) of m^3C and m^5C, respectively.

From the viewpoint of tRNA biogenesis, actin localization of Trm140p might be involved in hierarchical modification of tRNAs. Most of the modifications are introduced into tRNA precursors in the nucleus (Knapp et al. 1978; Phizicky and Hopper 2010), since many tRNA-modifying enzymes are localized there. Some modifications, however, can be introduced into tRNAs after export to the cytoplasm (Murthi et al. 2010). Considering the actin localization of Trm140p, m^3C formation should occur in the cytoplasm. In fact, $tRNA^{Thr1}$ and $tRNA^{Ser1}$ isolated from the *trm140Δ* strain contained most of the modifications other than m^3C32 (data not shown, pseudouridines were not analyzed), indicating that m^3C32 is introduced at the late step of tRNA biogenesis in the cytoplasm. This is consistent with our observation that the unmodified $tRNA^{Thr1}$ transcript was not as good a substrate for Trm140p, while the modified $tRNA^{Thr1}$ isolated from the *trm140Δ* strain was efficiently methylated by Trm140p. Hence, Trm140p might monitor tRNA maturation in the cytoplasm by recognizing other tRNA modifications.

Mass spectrometric analysis of individual tRNAs isolated from the *trm140Δ* strain revealed that *TRM140* is involved in m^3C formation in both $tRNA^{Thr1}$ and $tRNA^{Ser1}$. However, $tRNA^{Ser1}$ was not methylated by recombinant Trm140p in vitro under the same conditions that allow it to methylate $tRNA^{Thr1}$ (Fig. 5B). This suggests that there might be partner protein(s) for Trm140p that are required for it to recognize $tRNA^{Ser1}$ specifically. According to interactome analysis (Stark et al. 2011), there are 22 proteins that can associate with Abp140p (Trm140p). In addition, actin-binding proteins might also be candidates for partners of Trm140p. Further study will be necessary to clarify how $tRNA^{Ser1}$ is methylated by Trm140p. Otherwise, the order of modifications might be important for m^3C32 formation in $tRNA^{Ser1}$. Considering efficient m^3C32 formation in $tRNA^{Thr1}$ isolated from *trm140Δ* strain, there might be some modifications that act as positive determinants for m^3C32 formation in $tRNA^{Ser1}$.

Because position 32 of tRNA has an important role in accurate codon recognition, m^3C32 formation in $tRNA^{Thr1}$ or $tRNA^{Ser1}$ might play a role in modulating codon recognition and translational efficiency. No obvious phenotype of *trm140Δ* has been detected (Asakura et al. 1998), which indicates that this modification has no critical effect on translation. Recently, a chemical genetic approach was applied to characterize *S. cerevisiae* gene-deletion strains (Alamgir et al. 2010). In this study, a *trm140Δ* strain showed increased sensitivity to neomycin. Neomycin is an aminoglycoside antibiotic that targets the A-site decoding center on the small subunit of the ribosome. This result implies that the lack of m^3C32 might affect the A-site decoding in the presence of neomycin. In addition, it will be of value to test this strain under various stress conditions, including

nutrient deprivation, response to reactive oxygen species, and chemicals, to observe other phenotypes related to *ABP140*.

Another intriguing feature of *ABP140/TRM140* is the presence of an internal frameshift site (Asakura et al. 1998) at which the slippery sequence, CUUAGGC, can promote a 40% frameshift frequency (Belcourt and Farabaugh 1990; Shah et al. 2002; Farabaugh et al. 2006). This sequence was first identified as the +1 frameshift site of the *TYB* gene of the Ty1 retrotransposon (Kawakami et al. 1993; Voytas and Boeke 1993). On the 0-frame, the CUU and AGG codons are decoded by $tRNA^{Leu}$ and $tRNA^{Arg}$, respectively. However, the AGG codon frequently causes translational pausing at the A-site on the ribosome due to the low availability of $tRNA^{Arg}$ encoded by a single gene. During pausing, at the P-site, $tRNA^{Leu}$ bearing a UAG anticodon that recognizes the CUU codon, slips toward the +1 frame to base pair with the UUA codon. Then, the AGG codon for Arg is recoded as a GGC codon for Gly at the A site. Since replacing this frameshift site with the 0-frame sequence did not affect the expression of Trm140p and m^3C formation (Fig. 4), the functional importance of this recoding event is still enigmatic. If m^3C32 formation in $tRNA^{Thr1}$ or $tRNA^{Ser1}$ modulates its capacity for codon recognition and translational efficiency, it can be speculated that expression of Trm140p might be regulated by the efficiency of +1 frameshifing in its mRNA mediated by $tRNA^{Thr1}$ or $tRNA^{Ser1}$, with altered levels of m^3C modification at position 32. However, these tRNAs are not directly involved in the frameshift event. In addition, the frameshift site is only conserved in very close relatives of *S. cerevisiae* (Fig. 3B). Even if such regulation exists, its functional importance will be limited.

ABP140/TRM140 has a conserved Ado-Met binding motifs in its C-terminal region (Fig. 3A,B). Sequence alignment based on structural motif revealed that the Ado-Met binding motif in this protein belongs to a large family of Rossmann-fold type class I methyltransferases that consist of six conserved motifs (motifs I–VI) (Fig. 3B; Kozbial and Mushegian 2005). In motif II, a highly conserved acidic residue (Asp or Glu) corresponds to Asp466 in Trm140p. When Asp466 was replaced with Ala, no m^3C formation was observed (Fig. 4). According to structural analyses, this conserved Asp is located at the C terminus of β-strand 2 in Rossmann-fold-type class I methyltransferases (Martin and McMillan 2002; Kozbial and Mushegian 2005). In the crystal structure of rat glycine *N*-methyltransferase (GNMT) (Takata et al. 2003), the equivalent residue, Asp85, directly interacts with the 2′ and 3′ hydroxyl groups of ribose in Ado-Met via hydrogen bonds. In *E. coli*, when Asp277, which corresponds to Asp466 in Trm140p, was mutated in RsmC, a methyltransferase for N^2-methylguanosine at 1207 in 16S rRNA, its binding affinity for Ado-Met was lost (Sunita et al. 2007). This strongly suggests that Asp466 in Trm140p is directly involved in Ado-Met binding. Mutation of Asp547 to Ala decreased m^3C formation in the cell (Fig. 4). This Asp is not a conserved residue in motif VI of class I methyltransferases and might be involved in tRNA recognition. In addition, no activity of Trm140p was observed following deletion of the conserved C terminus (D602-Q621) (Fig. 4). This indicated that this region might be important for tRNA binding or protein folding. A series of mutation studies and kinetic analyses will be necessary to further characterize this enzyme. Moreover, it will also be worth attempting to obtain the crystal structure of Trm140p complexed with $tRNA^{Thr1}$.

MATERIALS AND METHODS

Strains, media, and plasmids

S. cerevisiae wild-type and deletion strains used in this study were obtained from EUROSCARF: the BY4742 (*Mat α; his3Δ1; leu2Δ0; lys2Δ0; ura3Δ0*) series and strains *yor239w*Δ and *yor240w*Δ (BY4742, *YOR239w::kanMX4*, and *YOR240w::kanMX4*). Yeast strain overexpressing hexahistidine-tagged Abp140p (YSC3869-9515832, Y258; Mat a; *pep4*Δ3; *his4*Δ580; *ura3*Δ53; *leu2*Δ3;/pABP140) was obtained from Open Biosystems. To construct the *abp140*Δ strain, the *ABP140* ORF was replaced with *URA3* by PCR-based gene deletion (Baudin et al. 1993). The PCR product was amplified from pCgURA3 (BYP1806 obtained from NBRP) as a template using the primers, 5′-ccaatacaattgtataccaaataagctattaca aattgatttaaatcgaggtcgacggtatc-3′ and 5′-cttgttttatgatgagagaggaggtg gtacttgtctcagaacttccgctctagaactagtggatc-3′. The Δ*pep4* strain obtained from EUROSCARF [BY4741; MATa; *his3* Δ 1; *leu2* Δ 0; *met15* Δ 0; *ura3* Δ 0; *pep4(YPL154c)::kanMX4*] was transformed with the PCR product. Ura+ transformants were selected to obtain the *abp140*Δ strain. Yeast strains were grown in rich medium (YPD: 2% peptone, 1% yeast extract, and 2% glucose) or in synthetic complete medium (SC: 0.67% yeast nitrogen base without amino acids, 0.5% casamino acid, and 2% glucose) supplemented with auxotrophic nutrients as specified. The plasmid pKT10-GAL-HA-ABP140 (Asakura et al. 1998) was used for expressing Abp140p in yeast cells.

Ribonucleome analysis

The procedure was performed as described previously (Noma et al. 2006; Suzuki et al. 2007). Briefly, yeast strains were grown in 5 mL of YPD in 24-well deep well plates at 30°C and the cells were harvested during log phase growth (OD_{660} = 1.5–2.0). Total RNAs were extracted from the cells of each gene-deletion strain by the phenolchloroform method. Approximately 20 μg of total RNA was digested to nucleosides and analyzed by LC/MS. Absence of a specific modified nucleoside was monitored on the mass chromatogram for each strain.

Isolation and purification of individual tRNAs from yeast

Reciprocal circulating chromatography was used to isolate individual tRNAs (Miyauchi et al. 2007). The sequences of the 3′-biotinylated DNA probes complementary to yeast $tRNA^{Thr1}$ and $tRNA^{Ser1}$ were 5′-tgcttccaatcggatttgaaccgatgatct-3′ and 5′-cgacacc agcaggatttgaaccagcgcggg-3′, respectively.

Mass spectrometry

RNA fragments digested by RNase T_1 were analyzed by LC/MS using ion-trap MS according to a previously described method (Kaneko et al. 2003; Noma et al. 2006), with slight modifications. Purified $tRNA^{Thr1}$ and $tRNA^{Ser1}$ (2.5 μg each) were subjected to digestion by RNase T_1 (Seikagaku corporation; 0.6 U) for 30 min at 37°C in a buffer of 10 mM NH_4OAc (pH 5.3). The hydrolysates were separated by ODS column chromatography (Xterra MS C18 2.5 μm, 2.1 x 50 mm, Waters). The solvent system consisted of 0.4 M 1,1,1,3,3,3-hexafluoro-2-propanol (pH 7.0, adjusted with triethylamine) in H_2O (Solvent A) and 50% methanol (Solvent B) with the following gradients: 5% B for 0–5 min, 5%–95% B for 5–35 min, 95% B for 35–40 min, 95%–5% B for 40–42 min, and 5% B for 42–60 min. The chromatographic effluent was directly conducted to the ESI source to ionize the separated RNA fragments, which were then analyzed on an LCQ DUO ion-trap mass spectrometer (ThermoElectron). Negative ions were scanned over an m/z range of from 620 to 2000 throughout the separation.

Expression and purification of the recombinant proteins

Yeast expressing hexahistidine-tagged Abp140p was grown at 30°C in YPD. Expression of recombinant proteins was induced by the addition of 2% galactose. After cultivation for 20 h, cells were harvested and washed with ddH_2O and then resuspended in lysis buffer (20 mM HEPES-KOH at pH 7.6, 10 mM KOAc, 2 mM $Mg(OAc)_2$, 1 mM dithiothreitol [DTT] and protease inhibitor cocktail [Roche]) and disrupted by five passes through a French press (Thermo Fischer Scientific). The cell lysate was cleared by ultracentrifugation at 100,000*g* for 1.5 h at 4°C. The hexahistidine-tagged protein was purified with the AKTA purifier chromatography system (GE Healthcare) using a Hi-Trap chelating HP column (GE Healthcare). Briefly, the column was washed once with ddH_2O and 10 mL of 0.1 M $NiSO_4$ was loaded on the column, followed by additional washes with ddH_2O. The column was then equilibrated with wash buffer (50 mM HEPES-KOH at pH 7.6, 100 mM KCl, 10 mM $MgCl_2$, 7 mM β-mercaptoethanol, and a protease inhibitor cocktail), and the cleared cell lysate was loaded onto the column and washed with 25–50 mL of wash buffer. The His-tagged proteins were eluted from the column with a linear-gradient of imidazole (50–450 mM) in wash buffer, and the eluted fractions were analyzed by SDS-PAGE. Fractions containing full-length Abp140p were pooled and dialyzed against a buffer containing 20 mM Tris-HCl (pH 7.6), 4 mM $MgCl_2$, 55 mM NaCl, and 1 mM DTT.

In vitro reconstitution of m^3C using recombinant Trm140p

The reaction mixture (10 μL) contained 50 mM Tris–HCl (pH 8.0), 0.5 mM DTT, 10 mM $MgCl_2$, 1 mM spermidine, 2 μg of $tRNA^{Thr1}$ or $tRNA^{Ser1}$ obtained from *yor240wΔ* strain, and 1.4 μM recombinant Abp140p, in the presence or absence of 0.5 mM Ado-Met. The reactions were incubated for 1 h at 30°C. After incubation, the reaction was stopped by the addition of neutralized phenol. $tRNA^{Thr1}$ or $tRNA^{Ser1}$ was extracted and precipitated by ethanol and then digested by nuclease P1 and bacterial alkaline phosphatase. RNA nucleoside analysis by LC/MS was carried out as described above.

RNA interference

Short hairpin RNAs (shRNAs) targeting hTrm140 and GFP (as a control) were designed by siExplorer and prepared as described (Katoh and Suzuki 2007). The sense strands of shRNAs for hTrm140 and GFP were 5′-GGAAGCAACUGACAAUGUA-3′ (shRNA-ABP140-1) and 5′-GGCACAAGCUGGAGUACAA-3′, respectively. The shRNAs were introduced into HeLa cells using Lipofectamine RNAiMAX (Invitrogen) as described previously (Katoh et al. 2009). Five days after transfection, the cells were harvested and total RNAs were extracted using TRIzol (Invitrogen). The steady-state level of hTrm140 mRNA was then measured by real-time RT–PCR using the primers 5′-ctcagcttcggtttaaaaaaggt-3′ and 5′-gtgtccagttcctcttgtgtg-3′, which confirmed that the level of hTrm140 mRNA was decreased to 8.8% of that of control cells transfected with GFP shRNA.

Site-directed mutagenesis

Site-directed mutagenesis of *ABP140* was carried out in the plasmid pKT10-GAL-HA-ABP140 (Asakura et al. 1998) with QuikChange Site-Directed Mutagenesis (Stratagene) according to the manufacturer's instructions. The introduced mutation in each construct was confirmed by DNA sequencing. The following pairs of oligonucleotides were used to create each mutation:

WT(0-frame), 5′-gttgatgactcttgtctaggcattgatcaacagca-3′ and 5′-tgctgttgatcaatgcctagacaagagtcatcaac-3′;
delN, 5′-gtaccggatccggtaccatgggcgatgctaccgttgatac-3′ and 5′-gtatcaacggtagcatcgcccatggtaccggatccggtac-3′;
D466A, 5′-gaggataatagccgcagcttttgctccaagagccg-3′ and 5′-cggctcttggagcaaaagctgcggctattatcctc-3′;
F481A, 5′-ttaaaaattctgaacaggccaaccccaagtacggcc-3′ and 5′-ggccgtacttggggttggcctgttcagaatttttaa-3′;
D547A, 5′-taagatcatatttcgtgcttacggtgcatatgatt-3′ and 5′-aatcatatgcaccgtaagcacgaaatatgatctta-3′;
K599A, 5′-taactcaagttagattcgcaaagaacagaatcctag-3′ and 5′-ctaggattctgttctttgcgaatctaacttgagtta-3′;
Y569A, 5′-tcctagaagagaacttcgccgttagaggtgatggta-3′ and 5′-taccatcacctctaacggcgaagttctcttctagga-3′;
del(D602-Q621), 5′-tggaaaataaaattggaactgctgtgtttgacgttcctca-3′ and 5′-tgaggaacgtcaaacacagcagttccaattttattttcca-3′.

SUPPLEMENTAL MATERIAL

Supplemental material is available for this article.

ACKNOWLEDGMENTS

We thank the members of the Suzuki laboratory, in particular Y. Sakaguchi, K. Miyauchi, and S. Kimura, for their technical support and many fruitful discussions. This work was supported by Grants-in-Aid for Scientific Research on Priority Areas from the Ministry of Education, Science, Sports, and Culture of Japan (to T.S.), by a JSPS Fellowship for Japanese Junior Scientists (to A.N.), and by a grant from the New Energy and Industrial Technology Development Organization (NEDO) (to T.S.).

Received January 31, 2011; accepted March 9, 2011.

REFERENCES

Agris PF, Vendeix FA, Graham WD. 2007. tRNA's wobble decoding of the genome: 40 years of modification. *J Mol Biol* **366:** 1–13.

Alamgir M, Erukova V, Jessulat M, Azizi A, Golshani A. 2010. Chemical-genetic profile analysis of five inhibitory compounds in yeast. *BMC Chem Biol* **10:** 6. doi: 10.1186/1471-6769-10-6.

Asakura T, Sasaki T, Nagano F, Satoh A, Obaishi H, Nishioka H, Imamura H, Hotta K, Tanaka K, Nakanishi H, et al. 1998. Isolation and characterization of a novel actin filament-binding protein from *Saccharomyces cerevisiae*. *Oncogene* **16:** 121–130.

Baudin A, Ozier-Kalogeropoulos O, Denouel A, Lacroute F, Cullin C. 1993. A simple and efficient method for direct gene deletion in *Saccharomyces cerevisiae*. *Nucleic Acids Res* **21:** 3329–3330.

Belcourt MF, Farabaugh PJ. 1990. Ribosomal frameshifting in the yeast retrotransposon Ty: tRNAs induce slippage on a 7 nucleotide minimal site. *Cell* **62:** 339–352.

Bjork GR. 1995. Biosynthesis and function of modified nucleosides. In *tRNA: Structure, biosynthesis and function*. Vol. 50, pp. 165–205. ASM Press, Herndon, VA.

Cantara WA, Crain PF, Rozenski J, McCloskey JA, Harris KA, Zhang X, Vendeix FA, Fabris D, Agris PF. 2011. The RNA Modification Database, RNAMDB: 2011 update. *Nucleic Acids Res* **39:** D195–D201.

Curran JF. 1998. Modified nucleosides in translation. In *Modification and editing of RNA: The alteration of RNA structure and function*. (ed. H Grosjean, R Benne), pp. 493–516. ASM press, Washington, DC.

Dunin-Horkawicz S, Czerwoniec A, Gajda MJ, Feder M, Grosjean H, Bujnicki JM. 2006. MODOMICS: a database of RNA modification pathways. *Nucleic Acids Res* **34:** D145–D149.

Farabaugh PJ, Kramer E, Vallabhaneni H, Raman A. 2006. Evolution of +1 programmed frameshifting signals and frameshift-regulating tRNAs in the order Saccharomycetales. *J Mol Evol* **63:** 545–561.

Guldener U, Munsterkotter M, Kastenmuller G, Strack N, van Helden J, Lemer C, Richelles J, Wodak SJ, Garcia-Martinez J, Perez-Ortin JE, et al. 2005. CYGD: the comprehensive yeast genome database. *Nucleic Acids Res* **33:** D364–D368.

Hall RH. 1963. Isolation of 3-methyluridine and 3-methylcytidine from solubleribonucleic acid. *Biochem Biophys Res Commun* **12:** 361–364.

Ikeuchi Y, Kimura S, Numata T, Nakamura D, Yokogawa T, Ogata T, Wada T, Suzuki T, Suzuki T. 2010. Agmatine-conjugated cytidine in a tRNA anticodon is essential for AUA decoding in archaea. *Nat Chem Biol* **6:** 277–282.

Iwanami Y, Brown GM. 1968. Methylated bases of ribosomal ribonucleic acid from HeLa cells. *Arch Biochem Biophys* **126:** 8–15.

Juhling F, Morl M, Hartmann RK, Sprinzl M, Stadler PF, Putz J. 2009. tRNAdb 2009: compilation of tRNA sequences and tRNA genes. *Nucleic Acids Res* **37:** D159–D162.

Kaneko T, Suzuki T, Kapushoc ST, Rubio MA, Ghazvini J, Watanabe K, Simpson L, Suzuki T. 2003. Wobble modification differences and subcellular localization of tRNAs in *Leishmania tarentolae*: implication for tRNA sorting mechanism. *EMBO J* **22:** 657–667.

Katoh T, Suzuki T. 2007. Specific residues at every third position of siRNA shape its efficient RNAi activity. *Nucleic Acids Res* **35:** e27. doi: 10.1093/nar/gkl100.

Katoh T, Sakaguchi Y, Miyauchi K, Suzuki T, Kashiwabara S, Baba T, Suzuki T. 2009. Selective stabilization of mammalian microRNAs by 3′ adenylation mediated by the cytoplasmic poly(A) polymerase GLD-2. *Genes Dev* **23:** 433–438.

Kawakami K, Pande S, Faiola B, Moore DP, Boeke JD, Farabaugh PJ, Strathern JN, Nakamura Y, Garfinkel DJ. 1993. A rare tRNA-Arg(CCU) that regulates Ty1 element ribosomal frameshifting is essential for Ty1 retrotransposition in *Saccharomyces cerevisiae*. *Genetics* **135:** 309–320.

Knapp G, Beckmann JS, Johnson PF, Fuhrman SA, Abelson J. 1978. Transcription and processing of intervening sequences in yeast tRNA genes. *Cell* **14:** 221–236.

Korostelev A, Noller HF. 2007. The ribosome in focus: new structures bring new insights. *Trends Biochem Sci* **32:** 434–441.

Kozbial PZ, Mushegian AR. 2005. Natural history of S-adenosylmethionine-binding proteins. *BMC Struct Biol* **5:** 19. doi: 10.1186/1472-6807-5-19.

Lustig F, Boren T, Claesson C, Simonsson C, Barciszewska M, Lagerkvist U. 1993. The nucleotide in position 32 of the tRNA anticodon loop determines ability of anticodon UCC to discriminate among glycine codons. *Proc Natl Acad Sci* **90:** 3343–3347.

Maden BE, Salim M. 1974. The methylated nucleotide sequences in HELA cell ribosomal RNA and its precursors. *J Mol Biol* **88:** 133–152.

Martin JL, McMillan FM. 2002. SAM (dependent) I AM: the S-adenosylmethionine-dependent methyltransferase fold. *Curr Opin Struct Biol* **12:** 783–793.

Miyauchi K, Ohara T, Suzuki T. 2007. Automated parallel isolation of multiple species of non-coding RNAs by the reciprocal circulating chromatography method. *Nucleic Acids Res* **35:** e24. doi: 10.1093/nar/gkl1129.

Murakami H, Ohta A, Suga H 2009. Bases in the anticodon loop of tRNA(Ala)(GGC) prevent misreading. *Nat Struct Mol Biol* **16:** 353–358.

Murthi A, Shaheen HH, Huang HY, Preston MA, Lai TP, Phizicky EM, Hopper AK. 2010. Regulation of tRNA bidirectional nuclear-cytoplasmic trafficking in *Saccharomyces cerevisiae*. *Mol Biol Cell* **21:** 639–649.

Nasvall SJ, Nilsson K, Bjork GR. 2009. The ribosomal grip of the peptidyl-tRNA is critical for reading frame maintenance. *J Mol Biol* **385:** 350–367.

Noma A, Kirino Y, Ikeuchi Y, Suzuki T. 2006. Biosynthesis of wybutosine, a hyper-modified nucleoside in eukaryotic phenylalanine tRNA. *EMBO J* **25:** 2142–2154.

Noma A, Sakaguchi Y, Suzuki T. 2009. Mechanistic characterization of the sulfur-relay system for eukaryotic 2-thiouridine biogenesis at tRNA wobble positions. *Nucleic Acids Res* **37:** 1335–1352.

Olejniczak M, Uhlenbeck OC. 2006. tRNA residues that have coevolved with their anticodon to ensure uniform and accurate codon recognition. *Biochimie* **88:** 943–950.

Olson MV, Page GS, Sentenac A, Piper PW, Worthington M, Weiss RB, Hall BD. 1981. Only one of two closely related yeast suppressor tRNA genes contains an intervening sequence. *Nature* **291:** 464–469.

Phizicky EM, Hopper AK. 2010. tRNA biology charges to the front. *Genes Dev* **24:** 1832–1860.

Riedl J, Crevenna AH, Kessenbrock K, Yu JH, Neukirchen D, Bista M, Bradke F, Jenne D, Holak TA, Werb Z, et al. 2008. Lifeact: a versatile marker to visualize F-actin. *Nat Methods* **5:** 605–607.

Shah AA, Giddings MC, Parvaz JB, Gesteland RF, Atkins JF, Ivanov IP. 2002. Computational identification of putative programmed translational frameshift sites. *Bioinformatics* **18:** 1046–1053.

Soma A, Ikeuchi Y, Kanemasa S, Kobayashi K, Ogasawara N, Ote T, Kato J, Watanabe K, Sekine Y, Suzuki T. 2003. An RNA-modifying enzyme that governs both the codon and amino acid specificities of isoleucine tRNA. *Mol Cell* **12:** 689–698.

Stark C, Breitkreutz BJ, Chatr-Aryamontri A, Boucher L, Oughtred R, Livstone MS, Nixon J, Van Auken K, Wang X, Shi X, et al. 2011. The BioGRID Interaction Database: 2011 update. *Nucleic Acids Res* **39:** D698–D704.

Sunita S, Purta E, Durawa M, Tkaczuk KL, Swaathi J, Bujnicki JM, Sivaraman J. 2007. Functional specialization of domains tandemly duplicated within 16S rRNA methyltransferase RsmC. *Nucleic Acids Res* **35:** 4264–4274.

Suzuki T. 2005. Biosynthesis and function of tRNA wobble modifications. In *Fine-tuning of RNA functions by modification and editing*, Vol. 12, pp. 24–69. Springer-Verlag, New York.

Suzuki T, Ikeuchi Y, Noma A, Suzuki T, Sakaguchi Y. 2007. Mass spectrometric identification and characterization of RNA-modifying enzymes. *Methods Enzymol* **425:** 211–229.

Takata Y, Huang Y, Komoto J, Yamada T, Konishi K, Ogawa H, Gomi T, Fujioka M, Takusagawa F. 2003. Catalytic mechanism of glycine N-methyltransferase. *Biochemistry* **42:** 8394–8402.

Voytas DF, Boeke JD. 1993. Yeast retrotransposons and tRNAs. *Trends Genet* **9:** 421–427.

Weissenbach J, Kiraly I, Dirheimer G. 1977. Primary structure of tRNA Thr 1a and b from brewer's yeast. *Biochimie* **59:** 381–391.

Yang HC, Pon LA. 2002. Actin cable dynamics in budding yeast. *Proc Natl Acad Sci* **99:** 751–756.